Annealing Effect on Dark Electrical Conductivity and Photoconductivity of Ga–In–Se Thin Films

M. Isik[a,*] and H.H. Gullu[b]

[a]Department of Electrical and Electronics Engineering, Atilim University, Ankara 06836, Turkey

[b]Department of Physics, Middle East Technical University (METU), Ankara 06800, Turkey

(Received January 26, 2016; in final form February 12, 2018)

Dark-conductivity and photoconductivity properties of thermally evaporated Ga–In–Se (GIS) thin films were investigated in the temperature range of 80–430 K. All measurements were performed on as-grown and annealed GIS thin films at 300 and 400 °C to get information about the effect of the annealing temperature on the conductivity properties. Room temperature conductivity was obtained as 1.8×10^{-8} Ω^{-1} cm^{-1} for as-grown films and increased to 3.6×10^{-4} Ω^{-1} cm^{-1} for annealed films at 400 °C. Analysis of the dark-conductivity data of as-grown films revealed nearly intrinsic type of conductivity with 1.70 eV band gap energy. Temperature dependent dark conductivity curves exhibited two regions in the 260–360 and 370–430 K for both of annealed GIS films. Conductivity activation energies were found as 0.05, 0.16 and 0.05, 0.56 eV for films annealed at temperatures of 300 and 400 °C, respectively. The dependence of photoconductivity on illumination intensity was also studied in the range from 17 to 113 mW/cm^2.

DOI: 10.12693/APhysPolA.133.1119

PACS/topics: 73.50.–h, 73.61.–r, 73.61.Jc

1. Introduction

GaSe and InSe compounds belonging to III–VI group semiconducting materials have been attractive especially in optoelectronic and photovoltaic applications [1–4]. Layered GaSe and InSe crystals are characterized by a highly anisotropic bonding forces. The reason of this high anisotropy is that the bonding within the layers is rather stronger than bonding perpendicular to layers. In GaSe and InSe, forces corresponding to interlayer interaction are predominantly of van der Waals type [5]. On the other hand, covalent bonding forces are effective within the layers. GaSe and InSe crystal structures consist of four monoatomic sheets in the order Se–Ga–Ga–Se and Se–In–In–Se, respectively [6–8]. GaSe has hexagonal structure with lattice parameters $a = 0.375$ and $b = 1.595$ nm (Joint Committee on Powder Diffraction Standard (JCPDS), Card no. 37-0931) and band gap energy of $\approx$ 2.0 eV [9]. The indirect transitions for thermally evaporated amorphous GaSe thin films were revealed as 1.8 eV [10] and 1.93 eV [11]. InSe crystals have indirect and direct band gap energies of $\approx$ 1.30 and 1.25 eV, respectively, at room temperature [12]. The optical characterization of thermally evaporated InSe thin films showed that room temperature direct band gap energies changes in the range of 1.21–1.38 eV depending on the substrate and annealing temperatures [6]. InSe crystals have hexagonal structure with lattice parameters of $a = 0.401$ and $b = 1.664$ nm (JCPDS, Card no. 34-1431). Researches indicated that GaSe have attractive properties to be used especially in nonlinear optical applications [2] whereas InSe is a promising material for photovoltaic conversions [13, 14].

$Ga_xIn_{1-x}Se$ mixed compounds are formed from the restricted combination of GaSe and InSe materials. Taking into consideration the role of constituent compounds in the technological applications, the mixed crystals can be thought as potential candidate to be used in photovoltaic, far-infrared conversion and nonlinear optical applications. Previous studies are restricted on the characterization of the bulk crystal forms of these mixed crystals. The optical characterization analysis on $Ga_xIn_{1-x}Se$ indicated that band gap energy increases from 1.2 eV ($x = 0$, InSe) to 2.0 eV ($x = 1$, GaSe) [15]. Our research group reported studies on the characterization of $Ga_{0.75}In_{0.25}Se$ ($x = 0.75$) crystals by means of optical absorption [16], ellipsometry [17], and dark electrical resistivity [18]. Moreover, in our previous work, we have reported optical properties of the thermally evaporated as-grown and annealed GIS thin films [19]. Analysis of transmission experiments performed in the 320–1100 nm wavelength range resulted in band gap energies between 1.52 and 1.65 eV depending on the annealing temperature. The aim of the present paper is to expand studies on Ga–In–Se films by investigating their dark conductivity and photoconductivity properties. The effect of annealing temperature on the conductivity properties of the films was also presented.

2. Experimental details

GIS films were grown onto ultrasonically cleaned soda-lime glass substrates by thermal evaporation of powdered $Ga_{0.75}In_{0.25}Se$ single crystals. The fine-grained GIS powder source was placed into an alumina coated tungsten boat. The thicknesses of the films grown at a evapo-

*corresponding author; e-mail: mehmet.isik@atilim.edu.tr

ration rate of about 1.0 Å/s were measured electromechanically around 1 μm by Dektak 6M thickness profilometer. GIS films were annealed at 300 and 400 °C for 30 min under nitrogen atmosphere. The chemical compositions of the deposited as-grown and annealed thin films were found using JSM-6400 scanning electron microscope. The atomic weight ratios of the constituent elements, Ga : In : Se, in all deposited films do not show significant changes and were around $\approx 34 : 16 : 50$. X-ray diffraction (XRD) measurements were performed using Rigaku Miniflex diffractometer with Cu K_α radiation ($\lambda = 0.154049$ nm) at a scanning speed of 0.02°/s. Four contacts were made on the film surface through suitable masks by thermal evaporation of pure indium (99.99%). Copper wires were connected to these contacts by silver paste. The contacts showed ohmic behavior verified from linearity of the current–voltage characteristics. The temperature-dependent conductivity measurements on the films grown in the van der Pauw geometry were accomplished in a closed cycle cryostat (Janis Liquid Nitrogen VPF series) in the temperature range of 80–430 K. Lakeshore 331 temperature controller was used to adjust and monitor the temperature of the samples. The photoconductivity measurements were carried out using halogen lamp illuminating the samples at different intensities in the range from 17 to 113 mW/cm^2.

3. Results and discussion

XRD technique was used to obtain structural parameters of the sample. X-ray diffractogram of as-grown (A0) and annealed GIS films at 300 °C (A1) and 400 °C (A2) present peaks at the same diffraction angle. However, peak intensities increase with annealing temperature. This is an indication of decrease of structural disorder and increase of crystallinity with increase of annealing temperature. Since the diffractograms are similar, we have only presented that of A2-film having most intensive peaks (see Fig. 1). The crystal system, the Miller indices of the diffraction peaks and lattice parameters were obtained using a least-squares computer program "DICVOL 04". Results revealed the crystal structure as tetragonal with lattice parameters of $a = 0.2873$ and $c = 1.6082$ nm. The Miller indices and diffraction angles of A2-films and constituent compounds, GaSe and InSe, are given in Table I. Diffraction angles of GIS thin film were recorded between those of GaSe and InSe. Most of the Miller indices of GIS films coincide with those of constituent compounds. Moreover, diffraction angles of thin films are closer to those of GaSe. This closeness can be attributed to the existence of higher composition of Ga atoms compared to In atoms in the thin film.

Figure 2 shows the temperature dependence of dark conductivity of deposited GIS films. It is seen that conductivity increases significantly for the A2-films compared to A1-films. The room temperature conductivities (σ_{room}) of the films increase from 1.8 $\times 10^{-8}$ Ω^{-1} cm^{-1} to 3.6 $\times 10^{-4}$ Ω^{-1} cm^{-1} (Table II).

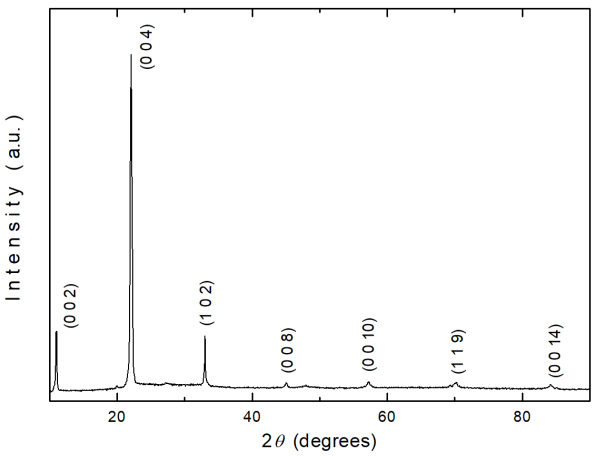

Fig. 1. X-ray powder diffraction pattern of A2-GIS thin films.

TABLE I

Comparison of the Miller indices and 2θ values of GIS thin film, GaSe, and InSe single crystals.

GIS thin film				GaSe[a]				InSe[b]			
h	k	l	2θ	h	k	l	2θ	h	k	l	2θ
0	0	2	11.00	0	0	2	11.10	0	0	2	10.60
0	0	4	22.10	0	0	4	22.30	0	0	4	21.30
1	0	2	33.05	0	0	6	33.80	0	0	6	32.25
0	0	8	45.05	0	0	8	45.50	0	0	8	43.50
0	0	10	57.25	0	0	10	57.80	0	0	10	55.20
1	1	9	70.10	0	0	12	70.90	0	0	12	67.50
0	0	14	84.20	0	0	14	85.40	0	0	14	80.90

[a]JCPDS, Card no. 37-0931, [b]JCPDS, Card no. 34-1431

The conductivity of the A2-films shows good agreement with the 4.5 $\times 10^{-4}$ Ω^{-1} cm^{-1} conductivity value of the $Ga_{0.75}In_{0.25}Se$ crystal which is the source material of the evaporation [19]. This consistency and higher conductivity can be attributed to the better crystallinity of the A2-films as observed from XRD pattern.

The dark conductivity data was analyzed to get information about the conductivity activation energies. Analysis showed that the data above 370 K for A0-films followed the relationship [20]:

$$\sigma = \sigma_0 \exp\left(-\frac{E_g}{2kT}\right), \tag{1}$$

where σ_0 is the pre-exponential factor and E_g is band gap energy. E_g value was found from the linear fit of

TABLE II

Room temperature conductivity (σ_{room}), band gap energy (E_g) and activation energies (ΔE) for as-grown and annealed GIS thin films.

Sample	σ_{room} [Ω^{-1} cm^{-1}]	E_g [eV]	ΔE_1 [eV]	ΔE_2 [eV]
A0	1.75 $\times 10^{-8}$	1.70	–	–
A1	1.20 $\times 10^{-7}$	–	0.56	0.05
A2	3.56 $\times 10^{-4}$	–	0.16	0.05

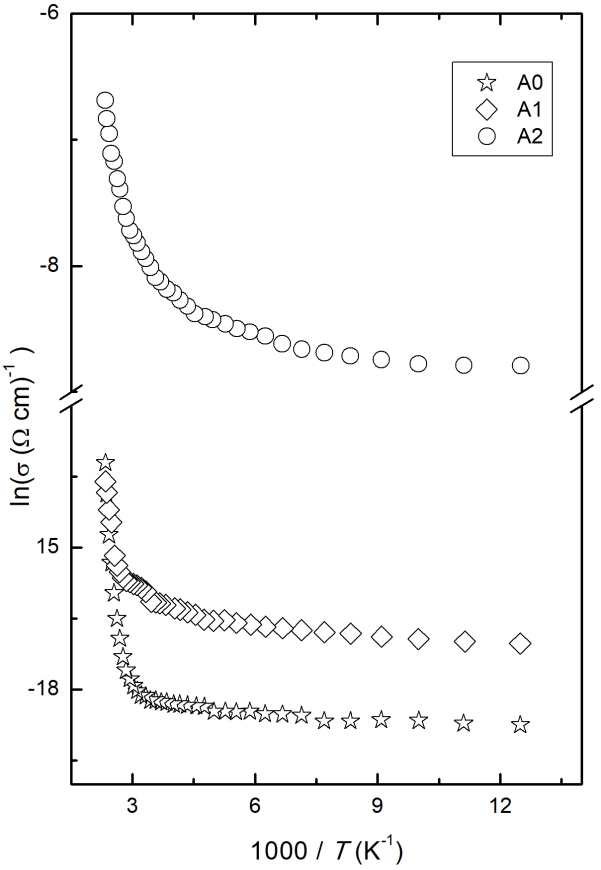

Fig. 2. Temperature dependence of conductivity of as-grown and annealed GIS thin films.

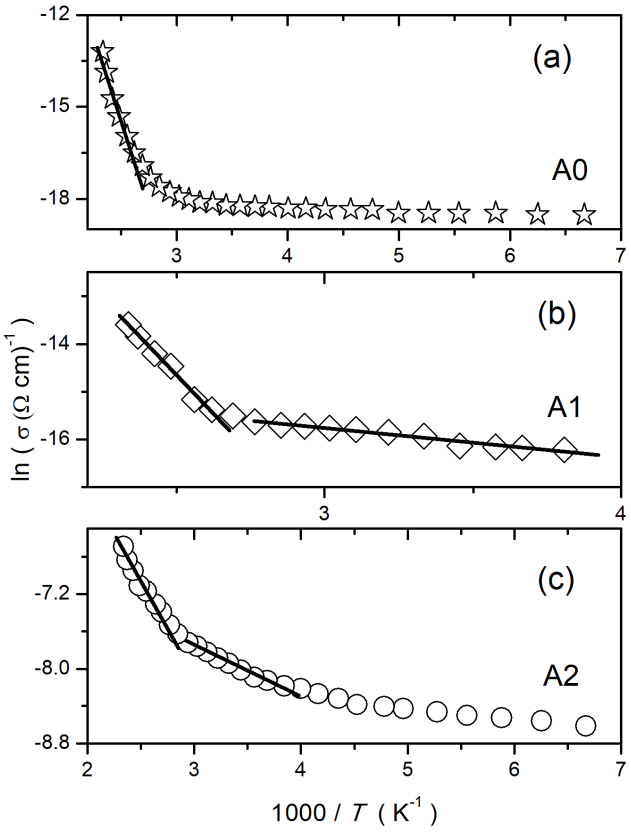

Fig. 3. Variation of $\ln(\sigma)$–T^{-1} for (a) A0-films, (b) A1-films and (c) A2-films. Solid lines represent the linear fits in the related temperature ranges.

the $\ln\,\sigma$ – $1000/T$ graph as 1.70 eV (see Fig. 3a). This value is in good agreement with 1.65 eV band gap energy obtained from the analysis of optical absorption measurements [19]. From this consistency, it can be thought that electrons excite from valence band to conduction band (intrinsic conductivity) above 370 K for A0-films. The energy of 1.70 eV for GIS film is between reported gap energies 1.80 and 1.3 eV of GaSe and InSe thin films, respectively [6, 12]. Moreover, gap energy of GIS thin film is closer to that of GaSe. This is an expected result since Ga composition is higher than In composition in the GIS thin films (Ga : 35.9%, In : 15.2%).

Temperature dependent conductivities of the annealed films were best analyzed under the light of extrinsic type of conduction expressed by the relation [20]:

$$\sigma = \sigma_0 \exp\left(-\frac{E_a}{kT}\right), \tag{2}$$

where E_a is the conductivity activation energy. Figure 3b and c show the relevant plots and linear fits for A1- and A2-films, respectively, to find the E_a energies. Both plots represent two different temperature regions of 260–370 K and 380–430 K. The E_a values related with these regions were obtained from the slopes as 0.05 and 0.56 meV for A1-films, 0.05 and 0.16 meV for A2-films. These values are significantly smaller than half of the band gap energy. This is a powerful indication of extrinsic type of conduction in annealed GIS thin films. These activation energies can be associated with different energy levels which may exist due to structural defects such as Ga, In and/or Se vacancies, interstitials and/or impurities arising through the growth process. As can be seen, the activation energy obtained for the 380–430 K region decreases as the annealing temperature increases. Since more free carriers are generated at any temperature in samples having higher conductivity, this decrease can be closely associated with the increase of conductivity with annealing temperature. Moreover, this decrease can also be attributed to an increase of crystallinity as considered in the results of XRD analysis. In the 260–370 K region, both annealed films give same activation energy which may possibly assigned to the same level and type of defect center.

Figure 4a–c shows the temperature dependent photoconductivities of films under different illumination intensities. As it is seen, conductivities of all films increase with light intensity. This increase is especially significant for A1-films whereas conductivity slightly increases for other films. Temperature dependence of conductivity in as-grown film shows two distinct temperature regions above and below 290 K. In the low temperature range of 80–290 K, conductivity at all light intensities are nearly

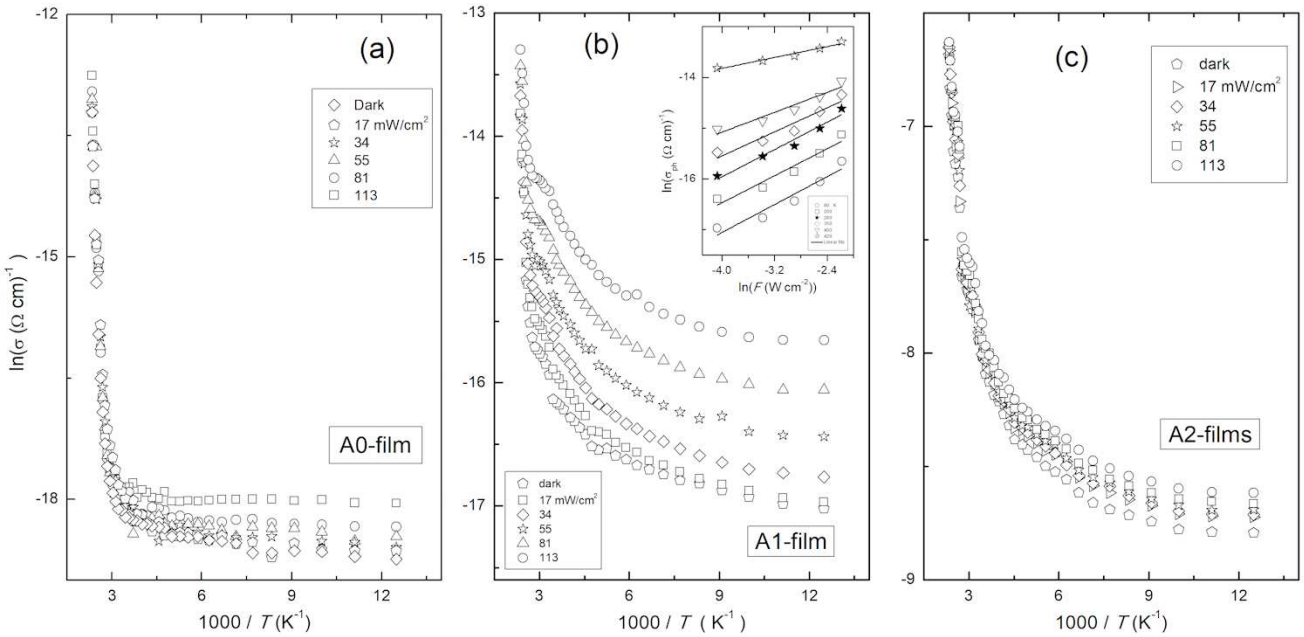

Fig. 4. Temperature dependence of photoconductivities of (a) A0-films, (b) A1-films, and (c) A2-films under different illumination intensities. Inset of (b): variation of photoconductivity with illumination intensity.

temperature independent whereas a sharp exponential increase with temperature was observed above 290 K. $\ln(\sigma)$ versus $1/T$ graphs for annealed films show similar temperature dependent regions as observed in temperature dependence of dark conductivity. Analysis of these regions under the light of Eq. (2) showed that conductivity activation energy decreases from 0.05 to 0.03 and 0.56 to 0.36 eV as light intensity increases for A1-films. The decrease of activation energy was also observed for A2-films in the high temperature region. Conductivity activation energy in the 380–430 K region decreased to 0.11 eV as light intensity increased to 113 mW cm^{-2}. However, E_a value in the low temperature region did not show a variation with illumination intensity.

The relation between photocurrent (I_{ph}) and illumination intensity (F) was investigated to get information about the nature of defect centers. Since conductivities of A0 and A2-films do not show remarkable dependence on illumination intensity, our interest focused on A1-films. Inset of Fig. 4b shows the variation of photocurrent with illumination intensity for some chosen temperatures. I_{ph} and F are related by $I_{ph} \propto F^n$, where the power exponent (n) gives information about the behavior of recombination mechanism. n values were calculated from the slopes of the linear fits (solid lines in inset of Fig. 4b) between 0.3 and 0.7. Material behaves as sublinear for $n < 1$ case meaning that lifetime of the free carrier increases and recombination at the surface becomes stronger with increase of the amount of conductive filler [21].

4. Conclusion

The conductivity properties of GIS films grown by thermal evaporation technique were investigated under dark and light with intensities in the range from 17 to 113 mW/cm^2. Measurements were carried out in the temperature range of 80–430 K on as-grown and annealed GIS films. The increase of the conductivity with annealing temperature and light intensity was observed in the present work. As-grown films introduced intrinsic conductivity with band gap energy of 1.70 eV in the temperature region above 370 K. Annealed GIS thin films exhibited two regions in the 260–360 and 370–430 K ranges in the temperature dependent dark conductivity measurements. Analysis of these regions resulted in 0.05–0.16 and 0.05–0.56 meV conductivity activation energies for films annealed at temperatures of 300 and 400 °C, respectively.

References

[1] S. Shigetomi, T. Ikari, *J. Appl. Phys.* **88**, 1520 (2000).

[2] N.B. Singh, D.R. Suhre, V. Balakrishna, M. Marable, R. Meyer, N. Fernelius, F.K. Hopkins, D. Zelmon, *Progr. Cryst. Growth Character. Mater.* **37**, 47 (1998).

[3] Y.Z. Lu, X.B. Wang, X.W. Zhu, X.L. Zhang, D.L. Zuo, Z.H. Cheng, *J. Appl. Phys.* **107**, 093105 (2010).

[4] A.G. Kyazym-zade, A.A. Agaeva, V.M. Salmanov, A.G. Mokhtari, *Tech. Phys.* **52**, 1611 (2007).

[5] R.H. Tregold, A. Clark, *Solid State Commun.* **7**, 1519 (1969).

[6] A. Chevy, A. Kuhn, M.S. Martin, *J. Cryst. Growth* **38**, 118 (1977).

[7] A. Seyhan, O. Karabulut, B.G. Akınoğlu, B. Aslan, R. Turan, *Cryst. Res. Technol.* **40**, 893 (2005).

[8] M.K. Anis, *J. Cryst. Growth* **55**, 465 (1981).

[9] S. Shigetomi, T. Ikari, H. Nakashima, *J. Appl. Phys.* **74**, 4125 (1993).

[10] K. Yilmaz, M. Parlak, C. Ercelebi, *Semicond. Sci. Technol.* **22**, 1268 (2007).

[11] B. Abidri, J.P. Lacharme, M. Ghamnia, C.A. Sebenne, M. Eddrief, M. Zerrouki, *Surf. Rev. Lett.* **6**, 1173 (1999).

[12] M. Ohyama, Y. Fujita, *Surf. Coat. Technol.* **169**, 620 (2003).

[13] S. Shigetomi, T. Ikari, H. Nakashima, *Phys. Status Solidi B* **209**, 93 (1998).

[14] T. Ishii, *J. Cryst. Growth* **89**, 459 (1988).

[15] L. Gouskov, A. Gouskov, M. Hajjar, L. Soonckindt, C. Llinares, *Physica B and C* **99**, 291 (1980).

[16] M. Isik, N.M. Gasanly, *Cryst. Res. Technol.* **47**, 530 (2012).

[17] M. Isik, S.S. Cetin, N.M. Gasanly, S. Ozcelik, *Solid State Commun.* **152**, 791 (2012).

[18] M. Isik, N.M. Gasanly, *Physica B* **421**, 53 (2013).

[19] M. Isik, H.H. Gullu, *Mod. Phys. Lett. B* **28**, 1450101 (2014).

[20] N.F. Mott, E.A. Davis, *Electronic Processes in Non-Crystalline Materials*, Oxford University Press, Oxford 1979.

[21] R.H. Bube, *Photoconductivity of Solids*, Wiley, New York 1960.